

Significantly Enhanced Red Photoluminescence Properties of Nanocomposite Films Composed of a Ferroelectric $\text{Bi}_{3.6}\text{Eu}_{0.4}\text{Ti}_3\text{O}_{12}$ Matrix and Highly *c*-Axis-Oriented ZnO Nanorods on Si Substrates Prepared by a Hybrid Chemical Solution Method

Hong Zhou, Xinman Chen, Guangheng Wu, Feng Gao, Ni Qin, and Dinghua Bao*

State Key Laboratory of Optoelectronic Materials and Technologies, School of Physics and Engineering, Sun Yat-Sen University, Guangzhou 510275, P. R. China

Received December 15, 2009; E-mail: stsbdh@mail.sysu.edu.cn

As one of the most promising candidate materials for nonvolatile ferroelectric memories, lanthanide-doped bismuth titanate [$\text{Bi}_{4-x}\text{Ln}_x\text{Ti}_3\text{O}_{12}$ (BLnT)] thin films have currently attracted tremendous interest. BLnT consists of a layered structure of $(\text{Bi}_2\text{O}_2)^{2+}$ and $(\text{Bi}_2\text{Ti}_3\text{O}_{10})^{2-}$ pseudoperovskite layers stacked along the *c*-axis direction. The lanthanide ions can substitute for the Bi ions in the pseudoperovskite layer and thus enhance the ferroelectric properties. On the other hand, BLnT thin films also show excellent optical properties. For example, $\text{Bi}_{3.25}\text{La}_{0.75}\text{Ti}_3\text{O}_{12}$ thin films exhibit remarkable optical nonlinearity,¹ and $(\text{Bi,Eu})_4\text{Ti}_3\text{O}_{12}$ (BEuT) thin films show the red photoluminescence (PL) properties of Eu^{3+} ions. In particular, the PL properties of BEuT thin films might have potential applications for integrated photoluminescent ferroelectric thin-film devices.² However, further enhancement of the emission intensity of BEuT is desirable.³

In this communication, we report our development of a hybrid chemical solution method for preparing nanocomposite films composed of a ferroelectric BEuT matrix and highly *c*-axis-oriented ZnO nanorods in an attempt to achieve a more efficient energy transfer from ZnO nanorods to Eu^{3+} ions in BEuT and thus to enhance the PL intensity of BEuT. Our study demonstrated that the nanocomposite films obtained exhibited significantly enhanced red PL properties. The energy transfer mechanism involved in the PL enhancement is also discussed.

The hybrid chemical solution method is described as follows: First, highly *c*-axis-oriented ZnO nanorods were obtained via a seed-layer solution growth approach. The seed layer was prepared by spin-coating a ZnO solution onto Si substrates followed by annealing at 600 °C for 1 h. The synthesis of the ZnO solution for seed-layer deposition was similar to that reported previously.⁴ Next, the Si substrates with the ZnO seed layers were immersed in a $\text{Zn}(\text{NO}_3)_2/\text{NH}_4\text{OH}$ aqueous solution at 90 °C for 20 min. Afterward, the samples were washed with deionized water and dried in air. Thus, the well-aligned ZnO nanorods were obtained on Si substrates (Figure 1d). The ZnO nanorods obtained were then coated with BEuT solution by a chemical solution deposition method using a spin-coating technique. The BEuT preparation process, including the solution synthesis, was similar to that in our previous report.² The samples were annealed at 700 °C for 1 h. Thus, the nanocomposite films composed of a BEuT matrix and highly *c*-axis-oriented ZnO nanorods were obtained (Figure 1f). For comparison, we also prepared individual BEuT films and ZnO nanorods on Si substrates under the same conditions.

Figure 1 shows X-ray diffraction (XRD) patterns and scanning electron microscopy (SEM) images of the nanocomposite film and individual ZnO nanorods on Si substrates. The XRD patterns show that the ZnO nanorods have excellent preferential *c*-axis orientation.

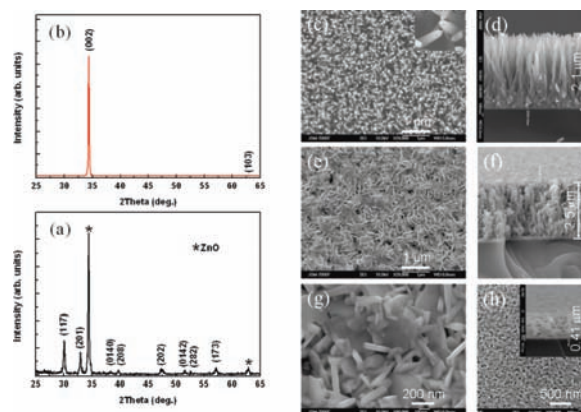


Figure 1. (left) XRD patterns of (a) a nanocomposite film and (b) ZnO nanorods on Si substrates. (right) SEM images: (c) surface and (d) cross section of ZnO nanorods; (e) surface and (f) cross section of the nanocomposite film; (g) a higher-magnification image of (e); (h) surface and (inset) cross section of an individual BEuT thin film. The difference in scales should be noted.

After being coated with BEuT, the ZnO nanorods still remain in the highly preferred *c*-axis orientation, whereas BEuT possesses a polycrystalline layered perovskite structure with random orientation. No secondary phases were detectable, indicating that the BEuT did not react with the ZnO nanorods after annealing at 700 °C. The SEM analysis indicates that the ZnO nanorods have a needlelike shape with a hexagonal tip and are well-aligned along the direction perpendicular to the substrate. The SEM images in Figure 1e,f also confirm that the nanocomposite film structure composed of the BEuT matrix and ZnO nanorods can be obtained by the hybrid chemical solution method. In Figure 1e, both mixed platelike and rodlike grains can be observed. To identify that the rodlike grains were not fractured ZnO nanorods, a higher-magnification SEM image was taken (Figure 1g), indicating clearly that the rodlike grains were also platelike ones but aligned in different directions or angles. Polycrystalline $(\text{Bi,Lu})_4\text{Ti}_3\text{O}_{12}$ thin films prepared by chemical solution deposition have also been reported to exhibit platelike grains.⁵ The SEM image in Figure 1h indicates that the BEuT thin film prepared under the same conditions had a thickness of ~410 nm, which is almost the same as the net thickness of BEuT in the nanocomposite film (~400 nm, as obtained from Figure 1d,f). In addition, the BEuT film exhibited a flat surface morphology in comparison with the nanocomposite film; this was due to different nucleation processes, since the former formed directly on the Si substrates whereas the latter nucleated on the *c*-axis-oriented ZnO nanorods.

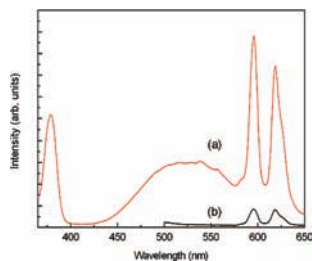


Figure 2. Emission spectra of (a) the nanocomposite film and (b) the BEuT thin film under 350 nm excitation.

Figure 2 shows emission spectra of (a) the nanocomposite film composed of the BEuT matrix and highly *c*-axis-oriented ZnO nanorods and (b) the BEuT thin film. The excitation wavelength was chosen as 350 nm, as the internal band excitation is more efficient than the intrinsic excitation of Eu^{3+} in BEuT host.² Compared with the individual BEuT thin film, the nanocomposite film comprising the BEuT matrix and ZnO nanorods exhibits much more intense emissions from Eu^{3+} ions, centered at 594 and 617 nm. The emission intensities were ~ 10 times stronger than those for the individual BEuT thin film. At the same time, in the emission spectrum, a sharp UV emission at ~ 380 nm and a broad emission centered at 525 nm were also observed. The former can be attributed to near-band-edge emission of ZnO, and the latter is commonly believed to originate from defect-related deep-level emission in ZnO, such as the radiative recombination of photogenerated holes with electrons occupying the oxygen vacancies.⁶ The existence of oxygen vacancies was confirmed by the appearance of the 583 cm^{-1} Raman peak (Figure S1a in the Supporting Information).

Comparing the emission spectrum of the nanocomposite film composed of the BEuT matrix and highly *c*-axis-oriented ZnO nanorods (Figure 2a) and the excitation spectrum of the BEuT thin film (Figure S2, left trace), we find that there are two spectral overlaps between the emission bands of the ZnO nanorods and the absorption bands of the Eu^{3+} ions in BEuT. One is the overlap between the sharp UV emission of ZnO at 380 nm and the ${}^7\text{F}_0 \rightarrow {}^5\text{L}_6$ transition of Eu^{3+} ions at 395 nm, and the other one is that between the defect-related deep-level emission band of ZnO centered at 525 nm and the ${}^7\text{F}_0 \rightarrow {}^5\text{D}_2$ transition of Eu^{3+} ions at 465 nm. It has been believed that energy transfer occurs only when the emission band of the sensitizer (ZnO in this study) overlaps spectrally with the absorption band of the activator (Eu^{3+} ions in this study). In our case, under the excitation of 350 nm radiation, ZnO nanorods first absorb the radiation energy and promote electrons to move from the valence band to the conduction band, leading to band-edge emission of ZnO. Next, as a result of the spectral overlap between the band-edge emission of the ZnO nanorods and the ${}^7\text{F}_0 \rightarrow {}^5\text{L}_6$ excitation spectrum of Eu^{3+} ions centered at 395 nm in BEuT, efficient energy transfer from the ZnO nanorods to the Eu^{3+} ions occurs, promoting the Eu^{3+} ions from the ${}^7\text{F}_0$ ground state to the ${}^5\text{L}_6$ excited state.⁷ The Eu^{3+} ions in the ${}^5\text{L}_6$ excited state undergo nonradiative decay to the ${}^5\text{D}_0$ state because the gaps between adjacent levels are small. Finally, a radiative transition between the ${}^5\text{D}_0$ and the ${}^7\text{F}_J$ ($J = 0-6$) states takes place because of the larger gap.^{7,8} This is one of the reasons that red PL of Eu^{3+} ions can be enhanced.

On the other hand, defect states such as oxygen vacancies in the ZnO nanorods also capture electrons, generating a broad green emission centered at 525 nm. Because of the spectral overlap between the defect-related emission of ZnO and the absorption band of the ${}^7\text{F}_0 \rightarrow {}^5\text{D}_2$ transition of Eu^{3+} ions at 465 nm, efficient energy transfer also occurs. Thus, some Eu^{3+} ions are promoted from the ${}^7\text{F}_0$ ground state to the ${}^5\text{D}_2$ excited state. Similarly, this can also result in enhancement of the red PL of Eu^{3+} ions. It has been reported that the defect states (trapping centers) in ZnO can temporarily store the excitation energy and then give rise to efficient energy transfer from the traps in ZnO to Eu^{3+} ions.⁹

For nonradiative energy transfer, the distance between the emission and absorption centers must be very close.⁷ Therefore, in Eu^{3+} -doped ZnO materials, the energy transfer is nonradiative.^{10,11} However, in our nanocomposite films, the energy transfer should be radiative because the BEuT matrix can only contact the outside part of the ZnO nanorods. It has been reported that in some other materials with Eu^{3+} as the activator combined with ZnO quantum dots or thin films, the energy transfer is radiative.^{7,12}

In conclusion, a significant enhancement of red photoluminescence has been demonstrated for nanocomposite thin films composed of a ferroelectric $\text{Bi}_{3.6}\text{Eu}_{0.4}\text{Ti}_3\text{O}_{12}$ matrix and highly *c*-axis-oriented ZnO nanorods on Si substrates prepared by a hybrid chemical solution method. The red-emission enhancement can be attributed to efficient radiation energy transfer from the ZnO nanorods to Eu^{3+} ions in the BEuT due to two spectral overlaps between the emission bands of ZnO nanorods and the absorption bands of Eu^{3+} ions in BEuT. Our study opens the possibility of realizing highly efficient photoluminescent ferroelectric multifunctional integrated thin-film devices. In addition, the hybrid chemical solution method also provides a useful route for the synthesis of some new nanocomposite thin films consisting of other inorganic matrixes and *c*-axis-oriented ZnO nanorods.

Acknowledgment. The authors gratefully acknowledge support from the NSFC (50872156, 10574164, and U0634006), FANEDD (200441), and NCET (06-0717).

Supporting Information Available: Measurement procedures, Raman spectra, and excitation and emission spectra. This material is available free of charge via the Internet at <http://pubs.acs.org>.

References

- (1) Shin, H.; Chang, H. J.; Boyd, R. W.; Choi, M. R.; Jo, W. *Opt. Lett.* **2007**, *32*, 2453.
- (2) Ruan, K. B.; Chen, X. M.; Liang, T.; Wu, G. H.; Bao, D. H. *J. Appl. Phys.* **2008**, *103*, 074101.
- (3) Ruan, K. B.; Chen, X. M.; Liang, T.; Wu, G. H.; Bao, D. H. *J. Appl. Phys.* **2008**, *103*, 086104.
- (4) Chen, X. M.; Wu, G. H.; Bao, D. H. *Appl. Phys. Lett.* **2008**, *93*, 093501.
- (5) Bao, D. H.; Chiu, T. W.; Wakiya, N.; Shinozaki, K.; Mizutani, N. *J. Appl. Phys.* **2003**, *93*, 497.
- (6) Chen, Y. W.; Liu, Y. C.; Lu, S. X.; Xu, C. S.; Shao, C. L.; Wang, C.; Zhang, J. Y.; Lu, Y. M.; Shen, D. Z.; Fan, X. W. *J. Chem. Phys.* **2005**, *123*, 134701.
- (7) Chong, M. K.; Abiyasa, A. P.; Pita, K.; Yu, S. F. *Appl. Phys. Lett.* **2008**, *93*, 151105.
- (8) Shionoya, S.; Yen, W. H. *Phosphor Handbook*; CRC Press: Boca Raton, FL, 1998; p 179.
- (9) Jia, W.; Monge, K.; Fernandez, F. *Opt. Mater.* **2003**, *23*, 27.
- (10) Yu, Y. L.; Wang, Y. S.; Chen, D. Q.; Huang, P.; Ma, E.; Bao, F. *Nanotechnology* **2008**, *19*, 055711.
- (11) Du, Y. P.; Zhang, Y. W.; Sun, L. D.; Yan, C. H. *J. Phys. Chem. C* **2008**, *112*, 12234.
- (12) Bang, J.; Yang, H.; Holloway, P. H. *J. Chem. Phys.* **2005**, *123*, 084709.

JA910388F